

Acinetobacter baumannii Strain M2 Produces Type IV Pili Which Play a Role in Natural Transformation and Twitching Motility but Not Surface-Associated Motility

Christian M. Harding,^{a,b} Erin N. Tracy,^a Michael D. Carruthers,^{a,b} Philip N. Rather,^c Luis A. Actis,^d Robert S. Munson, Jr.^{a,b}

Center for Microbial Pathogenesis, The Research Institute at Nationwide Children's Hospital, Columbus, Ohio, USA^a; Department of Pediatrics, College of Medicine, The Ohio State University, Columbus, Ohio, USA^b; Department of Microbiology and Immunology, Emory University, Atlanta, Georgia, and Research Service, Atlanta VA Medical Center, Decatur, Georgia, USA^c; Department of Microbiology, Miami University, Oxford, Ohio, USA^d

ABSTRACT *Acinetobacter baumannii* is a Gram-negative, opportunistic pathogen. Recently, multiple *A. baumannii* genomes have been sequenced; these data have led to the identification of many genes predicted to encode proteins required for the biogenesis of type IV pili (TFP). However, there is no experimental evidence demonstrating that *A. baumannii* strains actually produce functional TFP. Here, we demonstrated that *A. baumannii* strain M2 is naturally transformable and capable of twitching motility, two classical TFP-associated phenotypes. Strains were constructed with mutations in *pilA*, *pilD*, and *pilT*, genes whose products have been well characterized in other systems. These mutants were no longer naturally transformable and did not exhibit twitching motility. These TFP-associated phenotypes were restored when these mutations were complemented. More PilA was detected on the surface of the *pilT* mutant than the parental strain, and TFP were visualized on the *pilT* mutant by transmission electron microscopy. Thus, *A. baumannii* produces functional TFP and utilizes TFP for both natural transformation and twitching motility. Several investigators have hypothesized that TFP might be responsible, in part, for the flagellum-independent surface-associated motility exhibited by many *A. baumannii* clinical isolates. We demonstrated that surface-associated motility was not dependent on the products of the *pilA*, *pilD*, and *pilT* genes and, by correlation, TFP. The identification of functional TFP in *A. baumannii* lays the foundation for future work determining the role of TFP in models of virulence that partially recapitulate human disease.

IMPORTANCE Several investigators have documented the presence of genes predicted to encode proteins required for the biogenesis of TFP in many *A. baumannii* genomes. Furthermore, some have speculated that TFP may play a role in the unique surface-associated motility phenotype exhibited by many *A. baumannii* clinical isolates, yet there has been no experimental evidence to prove this. Unfortunately, progress in understanding the biology and virulence of *A. baumannii* has been slowed by the difficulty of constructing and complementing mutations in this species. Strain M2, a recently characterized clinical isolate, is amenable to genetic manipulation. We have established a reproducible system for the generation of marked and/or unmarked mutations using a modified recombineering strategy as well as a genetic complementation system utilizing a modified mini-Tn7 element in strain M2. Using this strategy, we demonstrated that strain M2 produces TFP and that TFP are not required for surface-associated motility exhibited by strain M2.

Received 11 May 2013 Accepted 9 July 2013 Published 6 August 2013

Citation Harding CM, Tracy EN, Carruthers MD, Rather PN, Actis LA, Munson RS, Jr. 2013. *Acinetobacter baumannii* strain M2 produces type IV pili which play a role in natural transformation and twitching motility but not surface-associated motility. mBio 4(4):e00360-13. doi:10.1128/mBio.00360-13.

Editor Ronald Taylor, Dartmouth Medical School

Copyright © 2013 Harding et al. This is an open-access article distributed under the terms of the [Creative Commons Attribution-Noncommercial-ShareAlike 3.0 Unported license](https://creativecommons.org/licenses/by-nc-sa/3.0/), which permits unrestricted noncommercial use, distribution, and reproduction in any medium, provided the original author and source are credited.

Address correspondence to Robert S. Munson, Jr., robert.munson@nationwidechildrens.org.

Acinetobacter baumannii is an aerobic Gram-negative, nonflagellated opportunistic pathogen; of late, some strains have developed resistance to most antimicrobial therapies (1). Hospital-acquired pneumonia is the most common clinical manifestation of *A. baumannii* infections; moreover, these infections frequently occur in mechanically ventilated patients, suggesting that environmental exposure to *A. baumannii* followed by subsequent accidental inoculation associated with the endotracheal tube may lead to infection (2). Interestingly, we now know that *A. baumannii* is not ubiquitous in nature but actually is isolated primarily within hospital settings on medical equipment, hospital workers, and patients and should not be considered just an environmental

contaminant (3). Key to *A. baumannii*'s persistence in hospital environments is its ability to resist desiccation, as it survives on surfaces, including bed rails, bedside tables, surfaces of ventilators, and even mattresses (4, 5). From 1993 to 2004, multidrug-resistant (MDR) *Acinetobacter* infections increased 23% in intensive care units, more than double the rate of any other Gram-negative bacillus (6). *A. baumannii* has gained attention as an "ESKAPE" pathogen, one of a cohort of microorganisms that cause the majority of MDR nosocomial infections within the United States, aptly named for their ability to escape the effects of modern antimicrobial therapies (7). Furthermore, the competency of *A. baumannii* to acquire antibiotic resistance genes has

now resulted in strains that are characterized as extensively drug resistant (XDR) and pan-drug resistant (PDR), prompting the suggestion that we may be nearing the end of the antibiotic era for this important Gram-negative pathogen (8, 9). In addition, the prevalence of MDR *A. baumannii*, an increase of infection incidence, and its recalcitrance to desiccation signifies the clinical importance of this opportunistic pathogen.

Although *A. baumannii* has earned global recognition for its ability to infect the immunocompromised patient population, little is actually known about how *A. baumannii* causes disease. Recent characterization of *A. baumannii* indicates that a few molecular factors are required for virulence in models that partially recapitulate human disease, including but not limited to outer membrane protein A (OmpA), phospholipase D, biofilm-associated protein (Bap), an O-glycosylation system, the *Acinetobacter* trimeric autotransporter (Ata), the Csu chaperone-usher type pilus, the acinetobactin-mediated iron acquisition system, and a secreted serine protease (10–18). Despite these significant findings, there is still a clear need to better define the bacterial determinants that facilitate colonization and subsequent disease.

Type IV pili (TFP) are multiprotein bacterial surface appendages assembled by many Gram-negative bacteria (19, 20). Due to their dynamic nature, TFP are able to be rapidly assembled and disassembled, participating in processes such as natural transformation, twitching motility, and adherence to abiotic and biotic surfaces. Natural transformation, or the ability of an organism to acquire exogenous DNA in a horizontal fashion, is a multistep process involving the uptake of DNA, processing of DNA, and ensuing homologous recombination (21). TFP-associated genes and their products are linked to DNA uptake; however, TFP alone are not sufficient for natural transformation. TFP also mediate a unique form of flagellum-independent motility termed twitching motility. Twitching motility involves the assembly of TFP, attachment of the pilus, and subsequent retraction of the pilus, facilitating the translocation of the cell body toward the point of attachment (22). Interestingly, the term “twitching motility” was coined in 1965 by Lautrop to describe the jerky locomotion exhibited by *Acinetobacter calcoaceticus*, thereby laying the foundation early for a link between *Acinetobacter* spp. and TFP (23).

Recently, Smith et al. sequenced the genome of *A. baumannii* strain ATCC 17978 and described several genes whose products might play a role in transformation; some of these were predicted to encode components of a TFP-like system (24). Furthermore, a recent analysis of the published *A. baumannii* genomes revealed many genes whose products have homology to proteins required for the biogenesis of TFP found in other Gram-negative bacteria; thus, it appears that some *A. baumannii* strains contain the coding potential required to assemble TFP (25). In addition to this analysis, Antunes et al. demonstrated that *A. baumannii* strain AYE exhibits twitching motility. A complete list of TFP biogenesis gene homologs in three *A. baumannii* reference strains can be found in the study by Antunes et al. (25). Eijkelkamp and coworkers simultaneously reported that several genes in *A. baumannii* strain ATCC 17978, which likely encode proteins required for TFP biogenesis, were slightly down-regulated under low-iron growth conditions and that surface-associated motility was lost (26). In other organisms, TFP are associated with numerous phenotypes, including natural transformation and/or twitching motility (27, 28). Ramirez et al. identified a clinical isolate of *A. baumannii* isolated from blood that was naturally transformable; however, the molec-

ular basis for this phenotype was not explored (29). Also, some *A. baumannii* clinical isolates are capable of twitching motility (reviewed in reference 30). Recently, Eijkelkamp et al. reported that all of the international clone I *A. baumannii* clinical isolates tested in their study as well as some clinical strains that did not belong to a currently characterized clonal lineage were capable of twitching motility, indicating that these strains may produce functional TFP (31). It has been speculated that TFP might play a role in the unique, flagellum-independent surface-associated motility displayed by many *A. baumannii* clinical isolates, yet there is no experimental evidence demonstrating that *A. baumannii* strains produce functional TFP (26, 32).

In this study, we demonstrated that *A. baumannii* strain M2, a clinical isolate, is naturally transformable and that natural transformation is dependent on genes which encode orthologs of proteins required for the biogenesis of TFP found in other Gram-negative organisms. These gene products were also required for twitching motility, another TFP-associated phenotype. Similar to observations made in other organisms (*Neisseria gonorrhoeae*, *Pseudomonas aeruginosa*, and *Dichelobacter nodosus*), the M2 Δ *pilT* mutant exhibited more surface-exposed PilA than the wild-type strain (33–35). TFP were readily visualized by transmission electron microscopy on *pilT* mutant cells but not on *pilA* or *pilA pilT* mutant cells. Collectively, these data led us to conclude that *A. baumannii* strain M2 produces functional TFP and that these structures are required for natural transformation and twitching motility. Lastly, we demonstrated that the unique surface-associated motility exhibited by many clinical isolates is not dependent on the production of functional TFP in strain M2.

RESULTS

Identification and arrangement of TFP biosynthesis gene clusters in *A. baumannii* strain M2. Roche 454 and Ion Torrent instruments were employed to obtain raw genomic sequence for strain M2. These data were assembled, and the resulting contig sets (R. S. Munson, Jr., and P. N. Rather, unpublished data) were queried for genes whose products have homology to proteins required for the biogenesis of TFP found in other Gram-negative organisms as well as in completed *A. baumannii* genomes. Antunes et al., in Table S2 of their article, published a list of putative TFP-associated genes in three *A. baumannii* genomes (25). Eijkelkamp and coworkers examined 11 fully sequenced *A. baumannii* genomes and reported that all contained genes likely to encode proteins involved in TFP biogenesis (31). In the strain M2 genome, we identified homologs of genes whose products are known to be critical in TFP biogenesis in other organisms. We chose three of these genes for further investigation, as our primary goal was to determine whether functional TFP are produced by strain M2. The TFP biogenesis-related gene clusters were arranged similarly to the gene clusters identified in other *A. baumannii* strains (25). One gene cluster was identified that contains genes that encode a putative traffic ATPase (PilB), a putative inner-membrane platform protein (PilC), and a putative prepilin peptidase (PilD) (Fig. 1). A second gene cluster contains genes that encode homologs of the TFP retraction ATPases PilT and PilU. A third locus contains a gene that encodes the putative major pilin subunit, PilA. PilA has a predicted six-amino-acid leader peptide, an N-terminal hydrophobic region, and a processed length of 138 amino acids (aa) (31). The protein has two cysteines, which are predicted to form one disulfide bridge. Together, these data indi-

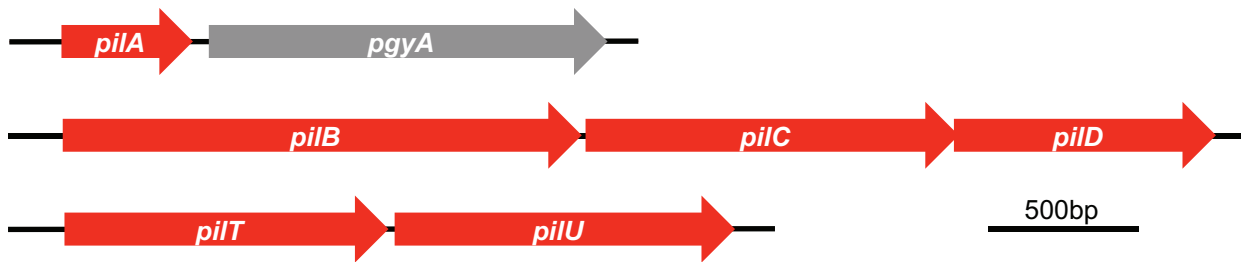


FIG 1 The *pil* gene loci in *A. baumannii* strain M2 employed in this study. Genes predicted to encode subunits of a TFP system in *A. baumannii* strain M2 are shown. We identified a *pilA* gene predicted to encode the major pilin subunit followed by *pgyA*, possibly coding for a type IV pilus O-glycosylase. Two other *pil* gene clusters were identified, (i) a *pilBCD* gene cluster, encoding a putative traffic ATPase (*pilB*), a putative inner membrane platform protein (*pilC*), and a putative prepilin peptidase (*pilD*), and (ii) a *pilTU* gene cluster, encoding two putative retraction ATPases.

cate that strain M2 has genes encoding a type IVa pilus system (36). The gene directly downstream of the *pilA* gene in strain M2 is predicted to encode a 436-aa hypothetical protein that contains a conserved Wzy_C domain found in the O-antigen ligase-like protein family. A gene encoding a member of the O-antigen ligase-like protein family is found immediately downstream of the *pilA* gene in some strains of *P. aeruginosa*. This Wzy_C domain-containing protein in *P. aeruginosa* is a pilin glycosylase (37). However, in the absence of functional data, we have designated the gene encoding this Wzy_C domain-containing protein in strain M2 *pgyA*, for “putative glycosylase A.”

The *pil* gene products were required for natural transformation. In addition to the identification of TFP-encoding genes, we observed that strain M2 was naturally transformable, a phenotype associated with the production of TFP in other naturally transformable Gram-negative organisms. We constructed strains containing mutations in the *pilA*, *pilD*, or *pilT* gene and then determined the transformation efficiency of each strain. As shown in Fig. 2, the transformation efficiency for all mutant strains was

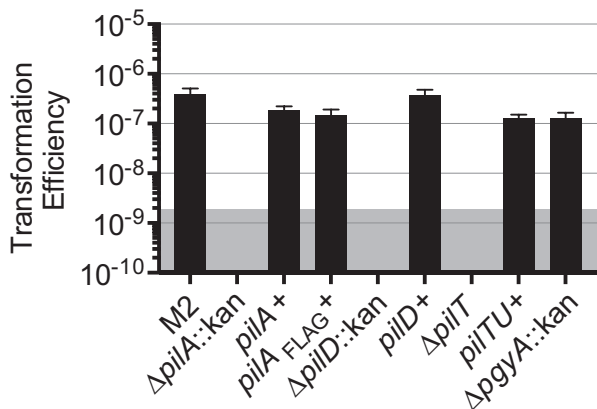


FIG 2 Natural transformation of strain M2 was reliant upon *pil* gene products. Strain M2, the *pilA*, *pilD*, and *pilT* isogenic mutants, and their respective complemented strains, including a Δ *pilA* strain complemented with the *pilA* gene fused to a FLAG tag, were tested for their transformation efficiencies. The *pilA*, *pilD*, and *pilT* mutants had transformation efficiencies below our level of detection, but the complemented strains, including the strain expressing PilA-FLAG, regained the natural transformation phenotype. The *pgyA* mutant also retained parental levels of transformation. The shaded area represents the level of detection of the assay. Transformation efficiency was calculated as the number of transformants/ml divided by the total CFU/ml for a given reaction. Bars show the means from three independent experiments with two technical replicates each, and error bars represent the standard errors of the means.

below the level of detection in our assay. Each mutation was complemented by cloning the parental gene under the control of its predicted native promoter into a mini-Tn7 element, which was then transposed into the *attTn7* site downstream of the *glmS2* gene in the strain M2 chromosome. Transformation levels similar to parental levels were observed in the complemented *pilA* and *pilD* mutants. In contrast, we were unable to complement the *pilT* mutation with the parental *pilT* allele. In *A. baumannii*, *pilT* and *pilU* are contiguous on the chromosome, as they are in *P. aeruginosa* (Fig. 1). However, in *P. aeruginosa*, *pilT* and *pilU* are independently transcribed, indicating that the promoter for *pilU* may be within the *pilT* open reading frame (34). Thus, it is likely that our inability to complement the *pilT* mutation was due to polar effects on *pilU*. We therefore reintroduced a complete *pilTU* gene cluster, using the mini-Tn7 system, into the *pilT* strain; the natural transformation phenotype was restored, suggesting that we may have affected transcription of *pilU* in the *pilT* mutant. In addition, we introduced an empty mini-Tn7 element into the *pilA* mutant and demonstrated that this strain did not have detectable levels of transformation, indicating that mini-Tn7 alone does not restore the transformation phenotype (Munson, unpublished data). We also generated a strain containing a deletion of the *pgyA* gene. This mutant was naturally transformable.

TFP-like structures were observed on the surface of strain M2. Type IV pili are long, narrow fibers, generally <8 nm in diameter, that can be readily visualized on the surface of many Gram-negative bacteria, including *Neisseria* species and *P. aeruginosa* (36). We failed to observe TFP-like structures when whole cells of strain M2 were examined by transmission electron microscopy (TEM). However, the inability to detect TFP by EM is similar to what we observed with TFP in *H. influenzae*; that is, unless the TFP regulon was overexpressed, TFP were not observed by EM (27). Others have demonstrated that strains containing mutations in the *pilT* gene of *N. gonorrhoeae*, *P. aeruginosa*, and *D. nodosus* are hyperpiliated compared to the parental strain (33–35). PilT is an ATPase that is required for disassembly of TFP; thus, bacteria with mutations in *pilT* are frequently observed to be hyperpiliated, as the pili cannot retract. Since pilus retraction is required for twitching motility and transformation, the pili observed in the *pilT* mutant are not functional. We readily observed TFP-like structures on the *pilT* mutant by TEM (Fig. 3). To verify that these structures were in fact TFP, we constructed a *pilT pilA* mutant strain and examined it for the loss of TFP-like structures. This strain was devoid of TFP-like structures, except for 1 cell out of the >1,000 viewed which displayed a structure with dimensions sim-

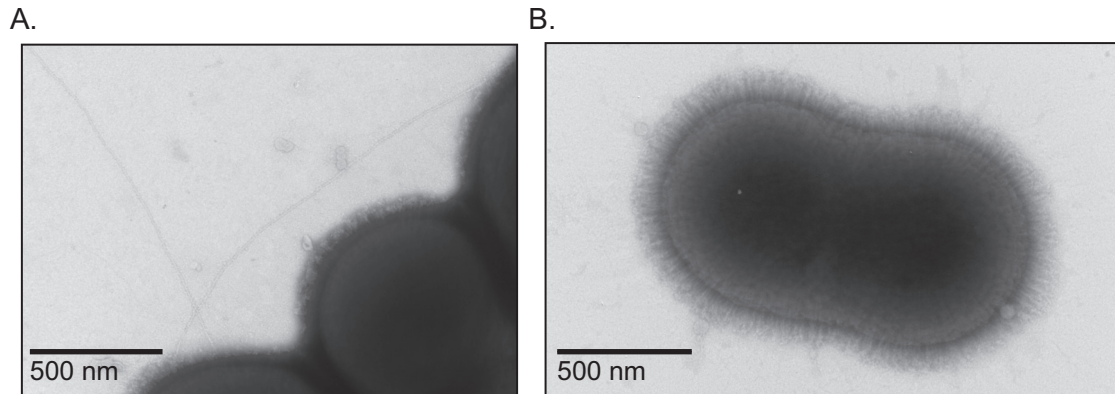


FIG 3 Observation of TFP on the $\Delta pilT$ mutant. (A) Type IV pilus-like appendages were readily observed on the surface of the $\Delta pilT$ mutant. (B) Type IV pilus-like appendages were not observed on the surface of a $\Delta pilT pilA::strAB$ mutant.

ilar to those of TFP. These data are consistent with the observed transformation phenotype in that both data sets affirm the conclusion that TFP are produced by strain M2.

The major pilin subunit, PilA, was surface exposed. Type IV pili are polymers composed predominately of the major pilin subunit, PilA, and minor pilins, so named for their relative abundance within the pilus fiber. By shearing pili from the surface of bacteria, the fiber can be separated from whole cells (38, 39), disassembled into its components, and separated by SDS-PAGE analysis, and protein composition can be determined via mass spectrometry. Cells of the parental M2 strain as well as the isogenic *pilA* and *pilT* mutant strains were vortexed to shear off surface structures. Whole cells were separated from the sheared protein fraction by centrifugation. The sheared protein fractions from each strain were then analyzed by SDS-PAGE. Selected bands were excised, and the proteins were identified by mass spectrometry. As shown in Fig. 4, when the sheared protein fractions were examined on a silver-stained SDS-PAGE gel, a band was present in the parental fraction slightly above the predicted mass of PilA (13.9 kDa). This band was absent in the fraction prepared from the *pilA* mutant. When preparations from the *pilT* mutant were characterized, a band which had the same mobility as the band in the parental fraction was observed. In addition, a band with a lower apparent molecular weight was present. The regions where the bands were present were excised from a Coomassie-stained SDS-PAGE gel, trypsinized, and subjected to MALDI-TOF (matrix-assisted laser desorption ionization–time of flight) mass spectrometry. As expected, the upper band present in the both the parental and *pilT* mutant fraction was identified as PilA. The PilA protein was not found in this region of the preparation from the *pilA* mutant. Interestingly, the lowest band in the *pilT* mutant fraction was also identified as PilA protein. These data taken together with the TEM images provide additional evidence that strain M2 produced TFP and that PilA is the major pilin subunit.

Lastly, a band running at an intermediate molecular weight between the upper and lower bands of the *pilT* mutant fraction was observed in all three samples. This band was identified as a protein containing a spore coat domain by Blast; however, structural prediction analysis (PHYRE2) (40) of the primary amino acid sequence revealed that this protein may be a pilin of a chaperone usher pilus system that is not yet characterized in *A. baumannii*. This protein is highly homologous to a putative biofilm

synthesis protein (NCBI accession number YP_001713377) found in *A. baumannii* strain AYE. We are currently investigating the role of this putative type I pilin in the biology of *A. baumannii*.

The strain M2 PilD homolog was required for processing of PilA. Based on homology, we predicted that *pilD* encodes the prepilin peptidase, a protein required in other TFP systems that acts by cleaving an N-terminal leader peptide from immature PilA. To test this prediction, we compared the apparent molecular weights of PilA proteins produced in *pilD*⁺ and *pilD* backgrounds. As we do not currently have an antiserum that recognizes strain

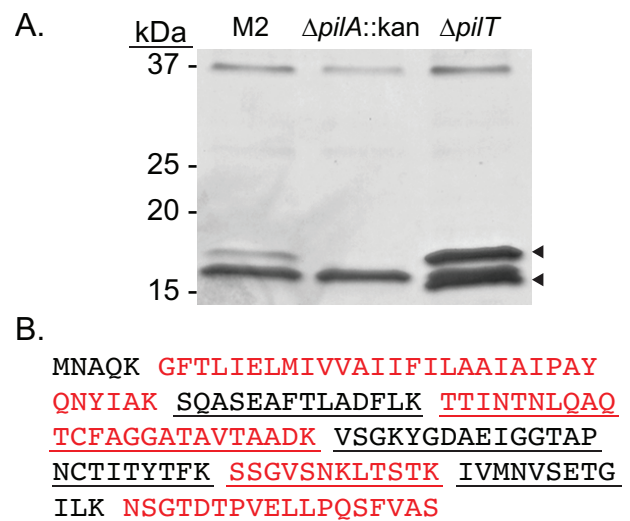


FIG 4 PilA, the major pilin subunit, is surface exposed. (A) The parental strain and the *pilA* and *pilT* mutant strains were resuspended in DPBS from L agar plates and vortexed to remove surface appendages. The sheared proteins were separated by SDS-PAGE, excised, and examined by MALDI-TOF mass spectrometry. The upper band in both the parental and *pilT* mutant fraction was identified as PilA. Interestingly, the lowest band present in the *pilT* mutant fraction was also identified as PilA. PilA was not identified in the *pilA* mutant fraction. (B) The primary amino acid sequence of the unprocessed prepilin, PilA, is shown. Predicted tryptic peptides are separated by spaces and shown in alternating colors for clarity. Underlined peptides were identified in both samples analyzed from the *pilT* mutant. The predominant band in the sample from the *pilA* mutant strain (also seen in the other preparations) is a predicted pilin produced by a chaperone/usher system. This is 87% identical to a putative biofilm synthesis protein (YP_001713377) in *A. baumannii* strain AYE.

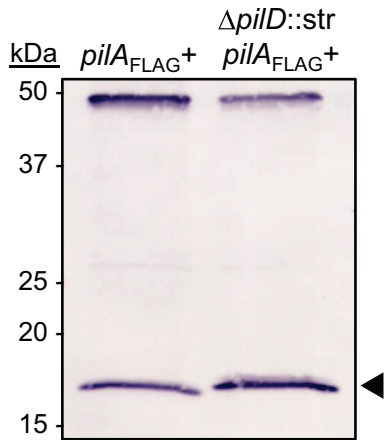


FIG 5 The strain M2 PilD homolog acted as a prepilin peptidase. Whole-cell lysates of the $M2\Delta pilA::kan(pilA-FLAG^+)$ and $M2\Delta pilA::kan\Delta pilD::strAB(pilA-FLAG^+)$ strains were examined by Western blot analysis for processed and unprocessed PilA-FLAG. The nonspecific band around 50 kDa was included to demonstrate equal migration of proteins. PilA-FLAG from the $M2\Delta pilA::kan(pilA-FLAG^+)$ migrated to a slightly lower position than PilA-FLAG from $M2\Delta pilA::kan\Delta pilD::strAB(pilA-FLAG^+)$. The leader peptide of PilA is predicted to be six amino acids.

M2's PilA, we constructed a mini-Tn7 element carrying sequence that encoded PilA with a C-terminal FLAG tag. Strains expressing the *pilA*-FLAG gene in a *pilA* and *pilA pilD* mutant background were constructed. We then compared whole-cell lysates of the two strains by Western blot analysis, probing with an anti-FLAG antibody. In Fig. 5, we show that PilA-FLAG was detected in both strains; however, PilA-FLAG from the *pilA pilD* mutant strain migrated as a higher-molecular-mass protein than PilA-FLAG produced in the *pilA* mutant background. These results are consistent with our hypothesis that PilD is the prepilin peptidase involved in processing of strain M2's major pilin, PilA.

The *pilA*, *pilD*, and *pilT* gene products were required for twitching motility but not surface-associated motility. Twitching motility, a TFP-dependent phenotype, is generally observed at the interphase of the petri dish and an agar or agarose surface. Given that transformation of strain M2 was dependent on TFP, we hypothesized that strain M2 would be capable of twitching motility. Classically, twitching motility assays have been conducted with medium containing 1% agar; however, agarose may be substituted. Media containing 1% agarose were used in these experiments. As shown in Fig. 6, strain M2 exhibited twitching motility. In contrast, the *pilA*, *pilD*, and *pilT* mutants did not exhibit twitching motility. Parental levels of twitching motility were observed when the complemented mutants were tested. The *pilA* mutant containing an empty mini-Tn7 element did not exhibit twitching motility (Munson, unpublished). The *pgyA* mutant strain retained parental levels of twitching motility.

Some *A. baumannii* isolates are also capable of a flagellum-independent surface-associated motility exhibited on semisolid media (41, 42). Clemmer et al. demonstrated that strain M2 was capable of surface-associated motility (32). In their study, surface-associated motility was impaired but not absent in a *pilT* mutant. To further explore the role of TFP in *A. baumannii* strain M2 surface-associated motility, we assessed the isogenic TFP mutant strains for their ability to translocate across the surface of semisolid media. Interestingly, the surface-associated motilities of the

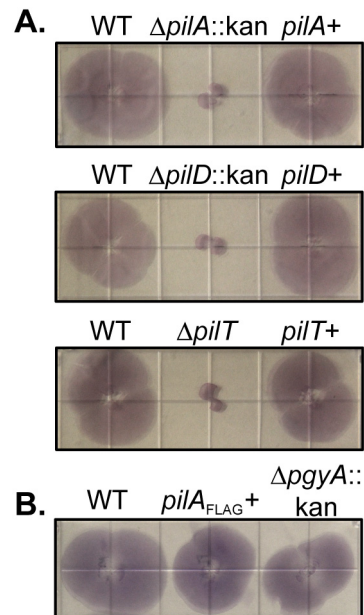


FIG 6 Twitching motility is reliant upon the *pil* gene products. (A) Twitching motility was observed at the agarose/plastic interface for M2 and the complemented mutants but not for the *pilA*, *pilD*, and *pilT* mutants. Each strain was inoculated by stabbing through the agarose to the surface of a plastic petri dish followed by incubation at 37°C for 18 h. The agarose was removed, and the nonadherent bacteria were removed by washing with PBS. The adherent bacteria were visualized by staining with 0.1% crystal violet. Each square in the grid on the plate is 13 mm wide. (B) The C-terminal FLAG tag on PilA did not impede twitching motility. The *pgyA* mutant retained the twitching motility phenotype.

pilA, *pilD*, and *pilT* mutants were similar to that of the parental M2 strain (Fig. 7).

DISCUSSION

Several investigators have noted that *A. baumannii* genomes contain genes that likely encode proteins required for the biogenesis

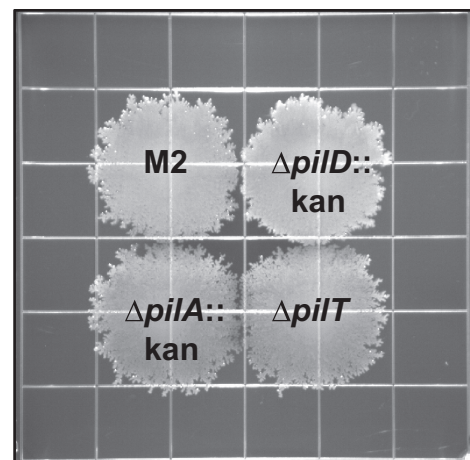


FIG 7 The *pil* gene products were not required for surface-associated motility. Strain M2 and the *pilA*, *pilD*, and *pilT* mutants were inoculated on the surface of a semisolid agarose plate (0.5%) and incubated for 18 h at 37°C. The *pilA*, *pilD*, and *pilT* mutant strains demonstrated no defect in surface-associated motility compared to the parental strain. Grids measure 13 mm².

of TFP, and it has been suggested that TFP might be involved in the surface-associated motility phenotype demonstrated by some *A. baumannii* isolates (32). We sought to definitively demonstrate the production of TFP in an *A. baumannii* clinical isolate and determine whether the classically defined TFP-associated phenotypes, transformation and twitching motility, required *A. baumannii* TFP.

In *A. baumannii* strain M2, we identified several genes whose products were known to be involved in TFP biogenesis in other organisms (27, 43). We demonstrated that strain M2 was naturally transformable and exhibited twitching motility; both phenotypes were absent in the *pilA*, *pilD*, and *pilT* mutants. The *pilA*, *pilD*, and *pilT* mutations were then complemented, restoring the TFP-dependent phenotypes.

Major and minor pilins are processed prior to being polymerized into a fiber by the removal of a leader peptide by a dedicated prepilin peptidase, PilD (44). We tested for the predicted PilD activity by constructing strains that expressed C-terminal FLAG-tagged PilA in a *pilA* mutant and a *pilA pilD* mutant background. When examined by Western blot, PilA-FLAG produced in the *pilA pilD* mutant ran with a slightly higher apparent molecular weight than the protein produced in the *pilD*⁺ strain, consistent with cleavage of the predicted six-amino-acid leader peptide.

Downstream of the *pilA* gene is a gene encoding a hypothetical protein containing an O-antigen ligase (Wzy_C) domain. This gene is found in a subset of genomes of the clinical isolates that have been sequenced. These include *A. baumannii* strain ACICU (accession no. CP000863), TYTH-1 (accession no. CP-003856), MDR-TJ (accession no. CP003500), MDR-ZJ06 (accession no. CP001937), TCDC-AB0715 (accession no. CP002522), and 1656-2 (accession no. CP001921). It is possible that PgyA is a pilin glycosylase, as PilO produced by *P. aeruginosa* 1244 also contains a Wzy_C domain, and catalyzes the addition of a trisaccharide to serine 148 of PilA (45). Eleven serine residues are present in the M2 PilA; however, the location of serines within the strain M2 protein are not the same as those identified as glycosylation targets in the *P. aeruginosa* 1244 pilin. Additional studies are required to determine the activity of PgyA.

The *pgyA* gene is not to be confused with the recently characterized *pglL* gene identified in *A. baumannii* ATCC 17978, although the *pglL* gene is present downstream of the *pilA* gene in strain ATCC 17978. In strains whose genomes contain the *pgyA* gene, the *pglL* gene is found immediately downstream of *pgyA*, as is the case in strain M2. In strain ATCC 17978, the *pglL* gene product is required for the O-glycosylation of several proteins of unknown function (14).

Type IV pili are surface appendages that have diameters ranging from 5 to 8 nm and can measure several micrometers in length. TFP have been visualized on, and purified from, many Gram-negative organisms (36). We employed numerous strategies to visualize TFP on the surface of strain M2, including using immunogold labeling and TEM to view pili on M2 strains expressing PilA-FLAG. These attempts were unsuccessful. However, when we examined the *pilT* mutant strain by negative-stain transmission electron microscopy, we were able to visualize structures emanating from the surface of the outer membrane that resembled TFP. These structures were present on a subset of the cells in the *pilT* mutant population and found free on the grid surface. In addition, these structures were rarely on the parent and absent in a *pilT pilA* mutant, indicating that these structures are most likely

TFP. These observations are expected, given the increase in relative abundance of surface exposed PilA on the *pilT* mutant compared to the parental M2 strain.

Enrichment for bacterial extracellular appendages by shearing bacteria in suspension without excessive cell lysis has been demonstrated for many organisms, including *P. aeruginosa* and non-typeable *H. influenzae* (27, 46). Therefore, sheared cell supernatants from the parental M2 as well as the *pilA* and *pilT* mutant strains were examined by Coomassie blue-stained SDS-PAGE. An additional band was present in the fraction from strain M2 when compared to the fraction from the *pilA* mutant. This same band was present in the fraction from the *pilT* mutant along with another lower molecular weight band which was absent in both the fraction from the strain M2 and the *pilA* mutant. Our observation was concordant with those obtained by Han et al., where a *pilT* mutant in *D. nodosus* demonstrated an increase in surface-exposed PilA compared to the parental strain (35). The upper band present in the fraction from the parent and the *pilT* mutant contained PilA when analyzed by MALDI-TOF mass spectrometry, confirming that strain M2 is able to export PilA to the surface of the cell and, by inference, assemble TFP. Interestingly, the lowest band in the fraction from the *pilT* mutant also contained PilA. We hypothesized that PilA in the lower band could simply be truncated or a proteolysis product; however, when we analyzed the mass spectrometry data for differential peptide identification, we found that the same peptides were present in both fractions. All peptides, with the exception of the hydrophobic amino terminal peptide, were present.

Genes predicted to encode TFP biogenesis proteins have been identified in all of the fully sequenced genomes of *A. baumannii* clinical isolates; however, most of the *A. baumannii* clinical isolates do not exhibit twitching motility (31), a classic phenotype associated with functional TFP. Additional work will be required to determine if the TFP-associated genes in these genomes are transcribed and under what conditions.

Recently, Eijkelkamp and coworkers reported that surface-associated motility and twitching motility were not always observed together and concluded that there are different mechanisms accounting for the different motility phenotypes displayed by *A. baumannii* clinical isolates (31). Twitching motility is a form of bacterial motility independent of flagella that requires the TFP to assemble, bind to a substratum, and then disassemble, resulting in movement of the cell body toward the point of attachment (22). Twitching motility was observed with strain M2, and this phenotype was dependent on the *pilA*, *pilD*, and *pilT* gene products, as twitching motility was absent in the mutant strains but restored to parental levels in the complemented strains. Eijkelkamp et al. demonstrated that there is sequence conservation between the PilA protein of *A. baumannii* clinical isolates within the same clonal lineage and that strains within the same clonal lineage exhibited similar motility patterns. Thus, their data suggested that specific PilA sequences might partially influence the ability of a strain to exhibit twitching motility. However, when we compared the sequence of strain M2's PilA to those identified in the study by Eijkelkamp et al., we found that M2's PilA sequence had 92% identity to that of *A. baumannii* strain 19606, a clinical isolate that did not exhibit twitching motility. Thus, it appears that PilA sequence does not correlate with ability of a particular strain to exhibit twitching motility.

Many strains of *A. baumannii* have also been shown to exhibit

a unique surface-associated motility on semisolid media that resembles swarming motility of *P. aeruginosa*; however, swarming motility, as defined by Henrichsen, is flagellum-coordinated movement of groups of cells across a solid surface (47). *Acinetobacter baumannii* surface-associated motility is a flagellum-independent, multifactorial, complex process that is partially dependent on 1,3-diaminopropane synthesis, quorum sensing, iron concentration, the composition of lipopolysaccharide and is sensitive to blue light when cells are grown at 24°C (30, 32, 41, 42). It has been speculated that TFP might be involved in the surface-associated motility of this bacterium. Recently, Clemmer et al. demonstrated, in strain M2, that a mutant deficient in expression of the PilT protein was partially impaired with respect to surface-associated motility (32). In contrast, the *pilT* mutant we characterized as well as the *pilA* and *pilD* mutants exhibited parental levels of surface-associated motility. Occasionally, the *pilD* mutant exhibited a variable motility compared to the parental strain as well as the other mutant strains. Rather and coworkers (unpublished data) have observed two subtle but distinct colony morphologies, opaque and translucent, when M2 is streaked on 1% L agar. These colony morphologies are independent of the TFP phenotype. When a translucent clone containing the *pilT* mutation was tested, surface-associated motility of the *pilT* mutant was impaired. In contrast, an opaque clone containing a *pilT* mutation retained parental levels of surface-associated motility. When streaked on a plate, colonies of the *pilT* mutant described by Clemmer et al. are primarily translucent (32). Colonies of the *pilT* mutant described herein were primarily opaque, which partially explains the discrepant results. Overall, however, it is clear that surface-associated motility is not strictly dependent on the expression of TFP in the opaque form. A complete understanding of the basis for the surface-associated motility will, in part, depend on the identification of the molecular basis for the translucent and opaque colony types.

Herein, we have provided genetic evidence that twitching motility and surface-associated motility are distinct phenotypes confirming and extending the observations of Eijkelkamp and coworkers (31). We also have demonstrated that PilA sequence does not correlate with the ability to exhibit twitching motility. Importantly, we have provided the first visual evidence of TFP production by an *A. baumannii* strain through the observation of TFP on the surface of the strain M2 *pilT* mutant, a phenotype that is dependent upon the *pilA* gene product. In addition, we demonstrated that PilA is a major surface-exposed protein, and taking these data together with the TEM images, we conclude that PilA is the major pilin subunit. Natural transformation and twitching motility were dependent on expression of TFP, while the mechanisms responsible for surface-associated motility remain to be determined; however, our data emphatically illustrate that TFP are not required for surface-associated motility of strain M2. Importantly, our study demonstrated that TFP are produced by and have a role in the biology of an *A. baumannii* clinical isolate. Future studies will be directed at defining the conditions that promote TFP expression and determining the role of TFP in the virulence of this emerging pathogen.

MATERIALS AND METHODS

Strains, plasmids, and growth conditions. Bacterial strains and plasmids used for this study are listed in Table S1 in the supplemental material. All bacterial strains were grown on L agar or in LB broth. When appropriate,

antibiotics were added to the *A. baumannii* cultures at the following concentrations: 750 µg ampicillin/ml, 20 µg kanamycin/ml, 50 µg streptomycin/ml, or 12.5 µg chloramphenicol/ml. When appropriate, *Escherichia coli* cultures were supplemented with antibiotics at the following concentrations: 50 µg ampicillin/ml for strains containing plasmids other than pGEM derivatives, 100 µg ampicillin/ml for strains containing pGEM derivatives, 25 µg streptomycin/ml, or 20 µg kanamycin/ml.

Construction of the *pilA*, *pilD*, and *pilT* mutants. Primers for this study were obtained from Integrated DNA Technologies (Coralville, IA) and are listed in Table S2 in the supplemental material. We constructed a mutant deficient in expression of the *pilA* gene as follows. The *pilA* gene plus approximately 1 kb of DNA 5' and 3' of *pilA* was amplified by PCR using primer set 1. The amplicon was then ligated into pGEM-T-Easy (Promega, Madison, WI), and the ligation products were transformed into *E. coli* DH5α. A plasmid with the correct insert was saved as pGEM-*pilA*, and the sequence of the insert was verified by sequencing. The *pilA* gene in pGEM-*pilA* was then replaced with a kanamycin resistance cassette flanked by FRT sites from pKD13 using a lambda recombinase-based strategy (48, 49). An amplicon was generated that contained 47 nucleotides (nt) of DNA 5' of *pilA* along with the translational start site, the cassette, the last 21 nt of the *pilA* gene and 29 nt downstream of *pilA* using primer set 2 and pKD13 as the template. The amplicon and pGEM-*pilA* were electroporated into *E. coli* strain DY380 that had been heat shocked at 42°C for 15 min prior to electroporation to induce expression of the lambda recombinase genes. Clones containing a plasmid with the *pilA* gene replaced by the cassette were identified on L agar supplemented with kanamycin. Plasmids were isolated and characterized; a plasmid containing FRT-*kan*-FRT (Flp recombination target) in place of the *pilA* gene was saved as pGEM- Δ *pilA*::*kan*.

Natural transformation was then used to move the Δ *pilA*::*kan* fragment into M2. The plasmid pGEM- Δ *pilA*::*kan* and primer set 1 were used to generate an amplicon containing Δ *pilA*::*kan* and flanked by 1 kb of DNA up- and downstream of *pilA*. An overnight culture of strain M2 was diluted 1:10 in 500 µl of LB broth and incubated at 37°C with shaking at 180 rpm for 2 h. Following the 2 h incubation, 1 µg of the amplicon was added to the bacterial culture. Cells were then transferred to an L agar plate and incubated at 37°C for 4 h. Cells were collected from the plate and resuspended in 500 µl of LB broth, and dilutions were plated on L agar supplemented with kanamycin at 37°C. Kanamycin-resistant clones were characterized by PCR analysis and sequencing to verify allele exchange. A clone was saved as M2 Δ *pilA*::*kan*. The identical strategy was used to construct M2 Δ *pilD*::*kan* using primer sets 3 and 4.

Since a mutation in *pilT* might be polar on *pilU*, we modified our strategy to remove the cassette, leaving a short open reading frame containing the translational start site of *pilT*, a small scar left by the excision of the cassette, and the last 21 nt of *pilT*. For this construction, *pilTU* were amplified from M2 genomic DNA with primer set 5 and cloned as described above. A clone was saved as pGEM-*pilTU*.

To construct an unmarked mutation in *pilT*, a derivative of pKD13 containing FRT-*kan-sacB*-FRT, pRSM3542, was used as the template in a PCR with primer set 6 (50). The amplicon, along with pGEM-*pilTU*, was electroporated into heat-shocked *E. coli* DY380 as described above. Restriction digest analysis and sequencing were performed on plasmid purified from kanamycin-resistant clones. A correct clone was saved as pGEM- Δ *pilT*::[*kan-sacB*] *pilU*. To introduce this mutation into strain M2, a PCR was performed using pGEM- Δ *pilT*::[*kan-sacB*] *pilU* as the template and primer set 5. This amplicon was introduced into strain M2 by natural transformation as described above. A kanamycin-resistant clone with the correct sequence was saved as M2 Δ *pilT*::*kan-sacB*.

A triparental mating strategy was employed to transiently introduce the pFLP2 plasmid, which expresses the FLP recombinase, into M2 Δ *pilT*::*kan-sacB* as described by Carruthers et al. (50). Briefly, 100 µl of stationary cultures normalized to an optical density at 600 nm (OD₆₀₀) of 2.0 of each of DH5α(pFLP2), HB101(pRK2013), and M2 Δ *pilT*::*kan-sacB* were added to 700 µl of warm LB broth. The bacterial suspension was washed twice by

centrifugation at $7,000 \times g$ followed by resuspension of the bacterial pellet in 1 ml of 32°C LB broth. On the final wash, the bacterial pellet was resuspended in 25 μ l of LB broth, and the suspension was spotted on a prewarmed L agar plate and incubated for 16 h at 32°C. The plates were then transitioned to 37°C for 2 h to transiently induce the FLP recombinase. Bacteria were then scraped from the plate and resuspended in 1 ml of LB broth. Serial dilutions were plated on L agar containing 10% sucrose and 12.5 μ g of chloramphenicol/ml and incubated at 26°C to select for transconjugants that had lost *sacB* and to select against *E. coli* strains. Strain M2 is naturally resistant to chloramphenicol at the concentrations used in this study. Clones demonstrating sucrose resistance were analyzed by PCR to verify loss of the *kan-sacB* cassette. A correct clone was sequenced and saved as M2 Δ *pilT*.

Construction of the *pgyA* mutant strain. The pGEM-*pilA* vector was constructed so that it contained the *pilA* gene as well as flanking DNA, which included the *pgyA* gene. Thus, to construct a *pgyA* mutant strain, the following strategy was employed. EcoRV, a unique restriction site 64 bp from the 5' end of *pgyA*, was used to digest pGEM-*pilA*. The kanamycin cassette from pUC4K was excised with HincII and ligated to the EcoRV-linearized pGEM-*pilA* and transformed into DH5 α , and clones were selected for on L agar supplemented with kanamycin. A clone demonstrating the correct restriction pattern was used to generate a PCR amplicon containing the interrupted *pgyA* gene along with approximately 1 kb of flanking DNA using primer set 1. The resulting amplicon was transformed into strain M2 via natural transformation as described above. Transformants were selected for on L agar supplemented with kanamycin. A clone with the correct insertion was verified with colony PCR and sequencing to confirm the mutation.

Construction of complemented mutant strains. A mini-Tn7 transposon system was used to complement mutations made in strain M2 in single copy, under the control of each gene's predicted promoter. Construction of the mini-Tn7-containing plasmid, pRSM3510, employed for this study has been described (50). The *pilA* gene along with 430 bp upstream of the start codon was amplified with primer set 7. The forward primer contained a BamHI site on the 5' end, while the reverse primer of each primer set contained KpnI on the 3' end. The amplicon was digested with BamHI and KpnI and ligated to pRSM3510 that had been digested with the same enzymes. The ligation mixture was electroporated into *E. coli* EC100D, and clones were selected on L agar containing ampicillin. Plasmids containing the *pilA* gene were identified by restriction digestion and verified by sequencing. A clone was saved as pRSM3510-*pilA*. Similarly pRSM3510-*pilTU*, which contains 312 bp upstream of the start codon of *pilT*, was constructed using primer set 8 with the following exceptions. The reverse primer did not have a KpnI site on the 3' end and was instead phosphorylated for use in a blunt cloning strategy. pRSM3510 was digested with BamHI and StuI, the *pilTU* amplicon was digested with BamHI, and the two were subsequently ligated together.

Since *pilD* is the last gene in a cluster of TFP-related genes (Fig. 1), we assumed that *pilD* transcription would be driven from a promoter 5' of *pilB*. Thus, we constructed a clone containing the putative *pilB* promoter driving expression of *pilD*. Plasmid pGEM-*pilBCD* was generated using primer set 3 and M2 genomic DNA as the template as described for pGEM-*pilA*. Inverse PCR using pGEM-*pilBCD* as the template and primer set 9 was utilized to create an in-frame deletion of *pilBC*, which left the putative promoter, the start codon of *pilB*, and the last 21 bp of *pilC* immediately 5' to the *pilD* gene. This amplicon was self-ligated and electroporated into DH5 α . Clones were selected for on L agar supplemented with ampicillin, and a plasmid containing the *pilBC* deletion was saved as pGEM-*pilD*. pGEM-*pilD* was used as a template in a PCR with primer set 10 to produce an amplicon that was cloned into pRSM3510 as described above for pRSM3510-*pilA*. Ligations were electroporated into EC100D, and clones were selected for on L agar supplemented with ampicillin. A correct clone was saved as pRSM3510-*pilD*.

Primer set 11 was used to amplify the template, pRSM3510-*pilA*, with a FLAG tag immediately upstream of the stop codon of the *pilA* gene. The

amplicon was self-ligated and electroporated into EC100D. Transformants were selected on L agar supplemented with ampicillin and a correct clone was sequence verified and saved as pRSM3510-*pilA*-FLAG.

Insertion of the mini-Tn7 constructs into the *A. baumannii* mutants. The pRSM3510 derivatives expressing the *pilA*, *pilD*, or *pilTU* genes were introduced into the respective *A. baumannii* M2 mutants via a four-parent conjugal strategy modified from that described by Kumar et al. (51). Briefly, 100 μ l of stationary cultures normalized to an OD₆₀₀ of 2.0 of the recipient strain (*A. baumannii* mutant), HB101(pRK2013), EC100D(pTNS2), and EC100D containing the appropriate pRSM3510 derivative were added to 600 μ l of warm LB broth. Each suspension was washed twice by centrifugation at $7,000 \times g$ followed by resuspension of the bacterial pellet in 1 ml of warm LB broth. On the final wash, the bacterial pellet was resuspended in 25 μ l of LB broth, and the suspension was spotted on a prewarmed L agar plate and incubated overnight at 37°C. The bacteria were scraped from the plate and resuspended in 1 ml of LB broth, vortexed for 8 s, and serial dilutions were plated on L agar plates supplemented with chloramphenicol to select against *E. coli* strains and ampicillin to select for *A. baumannii* strain M2 exconjugants that had received the mini-Tn7 constructs. To verify that mini-Tn7 had successfully transposed downstream of the *glmS2* gene, primer set 12 (Tn7L forward and downstream *glmS2* reverse) were used to amplify a 400-bp fragment that would produce a product only if mini-Tn7 had been inserted at the predicted *attTn7* in the correct orientation. The four strains were saved as M2 Δ *pilA*::*kan(pilA*⁺), M2 Δ *pilD*::*kan(pilD*⁺), M2 Δ *pilT*(*pilTU*⁺), and M2 Δ *pilA*::*kan(pilA*-FLAG⁺).

Construction of pGEM-*blsA*::*strAB*. The *blsA* gene along with 1 kb of upstream and downstream DNA was amplified by PCR with the primer set 13 using *A. baumannii* strain M2 genomic DNA as the template. The amplicon was A tailed, TA cloned into pGEM-T Easy, and electroporated into DH5 α . Transformants were selected on L agar supplemented with ampicillin, and correct clones were verified by restriction digestion and sequencing. The *strA* and *strB* genes along with approximately 400 bp of flanking DNA were amplified from *A. baumannii* strain RUH134 with the phosphorylated primer set 14. This PCR product was ligated to an EcoRV-digested pGEM-*blsA* and electroporated into DH5 α . Clones were selected for on L agar supplemented with streptomycin. A clone with the correct insertion was saved as pGEM-*blsA*::*strAB*. The interruption in the *blsA* gene is 72 bp downstream of the ATG start site.

Construction of the *pilT pilA* mutant. To construct a *pilT pilA* mutant, an insertionally inactivated *pilA* gene was introduced into the *pilT* mutant strain. Briefly, pGEM-*pilA* was used as the template to construct pGEM- Δ *pilA*, in which inverse PCR was performed using primer set 16 to create a deletion of *pilA*. A PCR product containing the streptomycin resistance genes *strAB* was amplified from RUH134 using primer set 14. The pGEM- Δ *pilA*- and *strAB*-containing PCR products were ligated together, and this ligation product was transformed into *E. coli* DH5 α . This plasmid was saved as pGEM- Δ *pilA*::*strAB*. The fragment containing Δ *pilA*::*strAB* was cut from pGEM- Δ *pilA*::*strAB* and cloned into pKNOCK-Km. This plasmid was saved as pKNOCK-Km- Δ *pilA*::*strAB*. *E. coli* EC100D cells harboring pKNOCK- Δ *pilA*::*strAB*, *E. coli* HB101 harboring pRK2013, and *A. baumannii* strain M2 Δ *pilT* were used as donor, helper, and recipient strains, respectively, in a triparental conjugation. Exconjugants containing Δ *pilA*::*strAB* were selected for on L agar containing chloramphenicol and streptomycin. Exconjugants were verified by PCR to confirm the *pilA* mutation. A verified clone was saved as M2 Δ *pilT* Δ *pilA*::*strAB*.

Construction of the *pilA pilD* mutant. To construct a *pilA pilD* mutant, we introduced a marked deletion of the *pilD* gene into the M2 Δ *pilA*::*kan(pilA*-FLAG⁺) strain via natural transformation. Briefly, pGEM-*pilBCD* was amplified by inverse PCR using primers set 15 to create an in-frame deletion of the *pilD* gene, in which the ATG start site as well as the last 21 nt of the *pilD* gene was left. The streptomycin cassette from *A. baumannii* RUH134 was amplified by PCR using primer set 14 which was 5' phosphorylated. The two amplicons were ligated and electroporated into

DH5 α , and clones were selected for on L agar plates containing streptomycin. A clone demonstrating the correct sequence was used to generate an amplicon encoding the *pilD* deletion interrupted with the streptomycin cassette as well as 1 kb of flanking DNA. The PCR product was transformed via natural transformation into the *pilA*-FLAG complemented *pilA* mutant as described above. A correct clone was verified by restriction digest and sequencing as M2 Δ *pilA::kan* Δ *pilD::strAB*(*pilA*-FLAG⁺).

Transformation efficiency assays. A single colony, from plates incubated overnight at 37°C, was used to inoculate 2 ml of LB broth. After overnight growth at 37°C and 180 rpm, 50 μ l of culture was diluted with 450 μ l of fresh LB broth and grown for 2 h at 37°C and 180 rpm. One microgram of pGEM-*blsA::strAB*, linearized with PstI, was added to cultures. After 2 h, the bacterium-DNA suspension was spotted on an L agar plate and incubated for 4 h at 37°C. Bacteria were removed from the plate, resuspended in 500 μ l LB broth, and normalized to an OD₆₀₀ of 50, and serial dilutions were plated on L agar to enumerate total CFU. In addition, serial dilutions were plated on L agar supplemented with streptomycin to enumerate CFU of transformants. Transformation efficiency was calculated by dividing the CFU of transformants by the total CFU. Experiments were conducted on at least three separate occasions.

Electron microscopy. M2 and the *pilA*, *pilT*, and *pilT pilA* mutant strains were streaked onto L agar and incubated overnight at 37°C. One hundred microliters of Dulbecco's phosphate-buffered saline (DPBS) was added to isolated colonies to create a slightly turbid bacterial suspension. Twenty microliters of the bacterial suspension was pipetted onto a piece of Parafilm, and a Formvar carbon film on 300 square mesh nickel grids (Electron Microscopy Sciences) was placed in each droplet for 5 min. The grids were blotted on filter paper and subsequently incubated in 20 μ l of 2% paraformaldehyde in DPBS for 1 h. The grids were washed three times in DPBS, blotted on filter paper, and then stained in a 2.0% (wt/vol) ammonium molybdate, 2.0% (wt/vol) ammonium acetate solution diluted 1:1 with deionized water for 5 min. The grids were blotted dry on filter paper and dried overnight. Images were captured on an FEI Tecnai G2 Spirit transmission electron microscope at the Campus Microscopy and Imaging Facility at The Ohio State University.

Pilus shear preparations. M2 and the *pilA* and *pilT* mutant strains were each streaked onto six L agar plates and incubated overnight at 37°C. In order to purify enough surface-exposed protein to visualize by Coomassie staining on a polyacrylamide gel, bacteria were collected from agar plates and resuspended in 5 ml of phosphate-buffered saline containing protease inhibitor cocktail (Roche), yielding a concentrated cell suspension. Appropriate dilutions were made, and cell suspensions were normalized via absorbance at 600 nm to an optical density of 50. Cells were vortexed at high speed for 1 min, followed by incubation on ice for 1 min. After centrifugation at 16,000 \times g for 1 min at 4°C, the resultant supernatants were removed, and ammonium sulfate was added to the supernatants to a final concentration of 30%. The preparations were incubated overnight at 4°C. The precipitated protein was then collected by centrifugation at 20,000 \times g and resuspended in 100 μ l of SDS-PAGE loading buffer. Twenty microliters of each sample was run in duplicate on a 4 to 20% TGX gel (Bio-Rad) for analysis by silver staining and Coomassie staining. Protein bands were excised and sent off for MALDI-TOF mass spectrometry analysis at the Campus Chemical Instrument Center Mass Spectrometry and Proteomics Facility at The Ohio State University.

Processed and unprocessed PilA-FLAG Western blots. To determine whether PilD was the leader peptidase, M2 Δ *pilA::kan*(*pilA*-FLAG⁺) and M2 Δ *pilA::kan* Δ *pilD::strAB pilA*(*pilA*-FLAG⁺) were streaked onto L agar and incubated for 16 to 18 h at 37°C. The cells were scraped from the plate into DPBS and normalized to an OD₆₀₀ of 5.0. Samples were resuspended in 1 \times loading buffer, boiled for 10 min, run on a 4 to 20% TGX gel, and transferred to nitrocellulose for Western blot analysis with an anti-FLAG antibody (Agilent) following the manufacturer's protocol.

Twitching motility. Twitching motility plates, comprised of 10 g tryptone/liter, 5 g NaCl/liter, and 10 g agarose/liter (BP164-100; Fisher), were prepared fresh for each experiment. Each plate was made by pouring 30

ml medium into a 150-mm petri dish and allowing the medium to air-dry with the lid off for 20 min in a laminar flow hood. Each twitching motility plate was stab inoculated with a colony of bacteria at the agarose/petri plate interface and placed in a 37°C, humidified incubator for 18 h. To visualize the bacteria at the interface, agarose was removed from each plate, and the plates were washed with phosphate-buffered saline (PBS) and stained with 0.1% crystal violet (wt/vol) in water for 5 min. To remove excess crystal violet, each plate was gently washed with PBS and allowed to dry. Twitching motility assays were conducted on at least three separate occasions.

Surface-associated motility. Surface motility plates, comprised of 5 g tryptone/liter, 2.5 g NaCl/liter, and 5 g agarose/liter (0.3%) as previously described (30), were prepared fresh for each surface motility experiment. In order to reduce variation between plates, each plate was poured with 30 ml of surface motility medium in a laminar flow hood with the lids off. The plates were allowed to dry for 30 min and then promptly used for motility assays. Motility plates were inoculated on the surface with 2 μ l of a bacterial suspension normalized to an OD₆₀₀ of 2.0. Each bacterial culture was started in the morning from an isolated colony and incubated to stationary phase at 37°C with shaking at 180 rpm. Motility plates were incubated for 18 h at 37°C. Surface-associated motility assays were conducted on at least three separate occasions.

SUPPLEMENTAL MATERIAL

Supplemental material for this article may be found at <http://mbio.asm.org/lookup/suppl/doi:10.1128/mBio.00360-13/-/DCSupplemental>.

Table S1, DOCX file, 0.2 MB.

Table S2, DOCX file, 0.1 MB.

ACKNOWLEDGMENTS

This work was supported by funds from the Research Institute at Nationwide Children's Hospital. C.M.H. was funded by the Howard Hughes Medical Institute Med into Grad Initiative.

REFERENCES

- Maragakis LL, Perl TM. 2008. Acinetobacter baumannii: epidemiology, antimicrobial resistance, and treatment options. *Clin. Infect. Dis.* 46:1254–1263.
- Dijkshoorn L, Nemec A, Seifert H. 2007. An increasing threat in hospitals: multidrug-resistant Acinetobacter baumannii. *Nat. Rev. Microbiol.* 5:939–951.
- Towner KJ. 2009. Acinetobacter: an old friend, but a new enemy. *J. Hosp. Infect.* 73:355–363.
- Weber DJ, Rutala WA, Miller MB, Huslage K, Sickbert-Bennett E. 2010. Role of hospital surfaces in the transmission of emerging health care-associated pathogens: norovirus, Clostridium difficile, and Acinetobacter species. *Am. J. Infect. Control* 38:S25–S33.
- Houang ET, Sormunen RT, Lai L, Chan CY, Leong AS. 1998. Effect of desiccation on the ultrastructural appearances of Acinetobacter baumannii and Acinetobacter lwoffii. *J. Clin. Pathol.* 51:786–788.
- Lockhart SR, Abramson MA, Beekmann SE, Gallagher G, Riedel S, Diekema DJ, Quinn JP, Doern GV. 2007. Antimicrobial resistance among gram-negative bacilli causing infections in intensive care unit patients in the United States between 1993 and 2004. *J. Clin. Microbiol.* 45:3352–3359.
- Rice LB. 2008. Federal funding for the study of antimicrobial resistance in nosocomial pathogens: no ESCAPE. *J. Infect. Dis.* 197:1079–1081.
- Hsueh PR, Teng LJ, Chen CY, Chen WH, Yu CJ, Ho SW, Luh KT. 2002. Pandrug-resistant Acinetobacter baumannii causing nosocomial infections in a university hospital, Taiwan. *Infect. Dis. 8:827–832.*
- Giamarellou H, Antoniadou A, Kanellakopoulou K. 2008. Acinetobacter baumannii: a universal threat to public health? *Int. J. Antimicrob. Agents* 32:106–119.
- Choi CH, Lee JS, Lee YC, Park TI, Lee JC. 2008. Acinetobacter baumannii invades epithelial cells and outer membrane protein A mediates interactions with epithelial cells. *BMC Microbiol.* 8:216.
- Lee JS, Choi CH, Kim JW, Lee JC. 2010. Acinetobacter baumannii outer membrane protein A induces dendritic cell death through mitochondrial targeting. *J. Microbiol.* 48:387–392.

12. Jacobs AC, Hood I, Boyd KL, Olson PD, Morrison JM, Carson S, Sayood K, Iwen PC, Skaar EP, Dunman PM. 2010. Inactivation of phospholipase D diminishes *Acinetobacter baumannii* pathogenesis. *Infect. Immun.* 78:1952–1962.
13. Brossard KA, Campagnari AA. 2012. The *Acinetobacter baumannii* biofilm-associated protein plays a role in adherence to human epithelial cells. *Infect. Immun.* 80:228–233.
14. Iwashkiw JA, Seper A, Weber BS, Scott NE, Vinogradov E, Stratilo C, Reiz B, Cordwell SJ, Whittall R, Schild S, Feldman MF. 2012. Identification of a general O-linked protein glycosylation system in *Acinetobacter baumannii* and its role in virulence and biofilm formation. *PLoS Pathog.* 8:e1002758. doi:10.1371/journal.ppat.1002758.
15. Bentancor LV, Camacho-Peiro A, Bozkurt-Guzel C, Pier GB, Mair-Litrán T. 2012. Identification of Ata, a multifunctional trimeric auto-transporter of *Acinetobacter baumannii*. *J. Bacteriol.* 194:3950–3960.
16. Tomaras AP, Dorsey CW, Edelmann RE, Actis LA. 2003. Attachment to and biofilm formation on abiotic surfaces by *Acinetobacter baumannii*: involvement of a novel chaperone-usher pili assembly system. *Microbiology* 149:3473–3484.
17. Gaddy JA, Arivett BA, McConnell MJ, López-Rojas R, Pachón J, Actis LA. 2012. Role of acinetobactin-mediated iron acquisition functions in the interaction of *Acinetobacter baumannii* strain ATCC 19606T with human lung epithelial cells, *Galleria mellonella* caterpillars, and mice. *Infect. Immun.* 80:1015–1024.
18. King LB, Pangburn MK, McDaniel LS. 2013. Serine protease PKF of *Acinetobacter baumannii* results in serum resistance and suppression of biofilm formation. *J. Infect. Dis.* 207:1128–1134.
19. Ayers M, Howell PL, Burrows LL. 2010. Architecture of the type II secretion and type IV pilus machineries. *Future Microbiol.* 5:1203–1218.
20. Mattick JS. 2002. Type IV pili and twitching motility. *Annu. Rev. Microbiol.* 56:289–314.
21. Chen I, Dubnau D. 2004. DNA uptake during bacterial transformation. *Nat. Rev. Microbiol.* 2:241–249.
22. Burrows LL. 2012. *Pseudomonas aeruginosa* twitching motility: type IV pili in action. *Annu. Rev. Microbiol.* 66:493–520.
23. Henrichsen J. 1983. Twitching motility. *Annu. Rev. Microbiol.* 37:81–93.
24. Smith MG, Gianoulis TA, Pukatzki S, Mekalanos JJ, Ornston LN, Gerstein M, Snyder M. 2007. New insights into *Acinetobacter baumannii* pathogenesis revealed by high-density pyrosequencing and transposon mutagenesis. *Genes Dev.* 21:601–614.
25. Antunes LC, Imperi F, Carattoli A, Visca P. 2011. Deciphering the multifactorial nature of *Acinetobacter baumannii* pathogenicity. *PLoS One* 6:e22674.
26. Eijkelkamp BA, Hassan KA, Paulsen IT, Brown MH. 2011. Investigation of the human pathogen *Acinetobacter baumannii* under iron limiting conditions. *BMC Genomics* 12:126.
27. Carruthers MD, Tracy EN, Dickson AC, Ganser KB, Munson RS, Jr, Bakaletz LO. 2012. Biological roles of nontypeable *Haemophilus influenzae* type IV pilus proteins encoded by the pil and com operons. *J. Bacteriol.* 194:1927–1933.
28. Skerker JM, Berg HC. 2001. Direct observation of extension and retraction of type IV pili. *Proc. Natl. Acad. Sci. U. S. A.* 98:6901–6904.
29. Ramirez MS, Don M, Merkier AK, Bistué AJ, Zorreguieta A, Centrón D, Tolmasky ME. 2010. Naturally competent *Acinetobacter baumannii* clinical isolate as a convenient model for genetic studies. *J. Clin. Microbiol.* 48:1488–1490.
30. Skiebe E, de Berardinis V, Morczinek P, Kerrinnes T, Faber F, Lepka D, Hammer B, Zimmermann O, Ziesing S, Wichelhaus TA, Hunfeld KP, Borgmann S, Gröbner S, Higgins PG, Seifert H, Busse HJ, Witte W, Pfeifer Y, Wilharm G. 2012. Surface-associated motility, a common trait of clinical isolates of *Acinetobacter baumannii*, depends on 1,3-diaminopropane. *Int. J. Med. Microbiol.* 302:117–128.
31. Eijkelkamp BA, Stroehrer UH, Hassan KA, Papadimitriou MS, Paulsen IT, Brown MH. 2011. Adherence and motility characteristics of clinical *Acinetobacter baumannii* isolates. *FEMS Microbiol. Lett.* 323:44–51.
32. Clemmer KM, Bonomo RA, Rather PN. 2011. Genetic analysis of surface motility in *Acinetobacter baumannii*. *Microbiology* 157:2534–2544.
33. Wolfgang M, Park HS, Hayes SF, van Putten JP, Koomey M. 1998. Suppression of an absolute defect in type IV pilus biogenesis by loss-of-function mutations in pilT, a twitching motility gene in *Neisseria gonorrhoeae*. *Proc. Natl. Acad. Sci. U. S. A.* 95:14973–14978.
34. Whitchurch CB, Mattick JS. 1994. Characterization of a gene, pilU, required for twitching motility but not phage sensitivity in *Pseudomonas aeruginosa*. *Mol. Microbiol.* 13:1079–1091.
35. Han X, Kennan RM, Davies JK, Reddacliff LA, Dhungyel OP, Whittington RJ, Turnbull L, Whitchurch CB, Rood JL. 2008. Twitching motility is essential for virulence in *Dichelobacter nodosus*. *J. Bacteriol.* 190:3323–3335.
36. Pelicic V. 2008. Type IV pili: e pluribus unum? *Mol. Microbiol.* 68:827–837.
37. Castric P. 1995. pilO, a gene required for glycosylation of *Pseudomonas aeruginosa* 1244 pilin. *Microbiology* 141:1247–1254.
38. Tramont EC, Sadoff JC, Boslego JW, Ciak J, McChesney D, Brinton CC, Wood S, Takafuji E. 1981. Gonococcal pilus vaccine. Studies of antigenicity and inhibition of attachment. *J. Clin. Invest.* 68:881–888.
39. Schoolnik GK. 1994. Purification of somatic pili. *Methods Enzymol.* 236:271–282.
40. Kelley LA, Sternberg MJ. 2009. Protein structure prediction on the Web: a case study using the Phyre server. *Nat. Protoc.* 4:363–371.
41. Mussi MA, Gaddy JA, Cabruja M, Arivett BA, Viale AM, Rasia R, Actis LA. 2010. The opportunistic human pathogen *Acinetobacter baumannii* senses and responds to light. *J. Bacteriol.* 192:6336–6345.
42. McQueary CN, Kirkup BC, Si Y, Barlow M, Actis LA, Craft DW, Zurawski DV. 2012. Extracellular stress and lipopolysaccharide modulate *Acinetobacter baumannii* surface-associated motility. *J. Microbiol.* 50:434–443.
43. Rudel T, Facius D, Barten R, Scheuerpflug I, Nonnenmacher E, Meyer TF. 1995. Role of pili and the phase-variable PilC protein in natural competence for transformation of *Neisseria gonorrhoeae*. *Proc. Natl. Acad. Sci. U. S. A.* 92:7986–7990.
44. Strom MS, Nunn DN, Lory S. 1993. A single bifunctional enzyme, PilD, catalyzes cleavage and N-methylation of proteins belonging to the type IV pilin family. *Proc. Natl. Acad. Sci. U. S. A.* 90:2404–2408.
45. Comer JE, Marshall MA, Blanch VJ, Deal CD, Castric P. 2002. Identification of the *Pseudomonas aeruginosa* 1244 pilin glycosylation site. *Infect. Immun.* 70:2837–2845.
46. Baynham PJ, Ramsey DM, Gvozdyev BV, Cordonnier EM, Wozniak DJ. 2006. The *Pseudomonas aeruginosa* ribbon-helix-helix DNA-binding protein AlgZ (AmrZ) controls twitching motility and biogenesis of type IV pili. *J. Bacteriol.* 188:132–140.
47. Henrichsen J. 1972. Bacterial surface translocation: a survey and a classification. *Bacteriol. Rev.* 36:478–503.
48. Datsenko KA, Wanner BL. 2000. One-step inactivation of chromosomal genes in *Escherichia coli* K-12 using PCR products. *Proc. Natl. Acad. Sci. U. S. A.* 97:6640–6645.
49. Tracy E, Ye F, Baker BD, Munson RS, Jr. 2008. Construction of non-polar mutants in *Haemophilus influenzae* using FLP recombinase technology. *BMC Mol. Biol.* 9:101.
50. Carruthers MD, Nicholson PA, Tracy EN, Munson RS, Jr. 2013. *Acinetobacter baumannii* utilizes a type VI secretion system for inter-bacterial competition. *PLoS One* 8:e59388. doi:10.1371/journal.pone.0059388.
51. Kumar A, Dalton C, Cortez-Cordova J, Schweizer HP. 2010. Mini-Tn7 vectors as genetic tools for single copy gene cloning in *Acinetobacter baumannii*. *J. Microbiol. Methods* 82:296–300.